DOI: 10.1002/ejic.200800436

Synthesis, Characterization, and *cis–trans* Isomerization Studies of *cis*-[$PdCl_2${$Ph_2P(CH_2CH_2O)_3CH_2CH_2PPh_2$-P,P′}] and *trans*-[$PtCl_2${$Ph_2P(CH_2CH_2O)_3CH_2CH_2PPh_2$-P,P′}] Metallacrown Ethers

Samuel B. Owens Jr.,[a] Dale C. Smith Jr.,[b] Charles H. Lake,[c] and Gary M. Gray*[a]

Keywords: Isomerization / Platinum / Palladium / Crown ethers

The metallacrown ether *cis*-[$PdCl_2${$Ph_2P(CH_2CH_2O)_3CH_2CH_2PPh_2$-P,P′}] (*cis*-**1**) has been kinetically trapped via precipitation during the reaction of $PdCl_2$ and $Ph_2P(CH_2CH_2O)_3CH_2CH_2PPh_2$ in an acetonitrile/THF mixture. The kinetics of the *cis–trans* isomerization and oligomerization equilibria of *cis*-**1** have been followed using quantitative $^{31}P\{^1H\}$ NMR spectroscopy. The reaction follows reversible first-order kinetics, and an Eyring analysis was carried out to yield $\Delta H^{\ddagger}_f$ (81 ± 2 kJ mol^{-1}), $\Delta H^{\ddagger}_r$ (46 ± 2 kJ mol^{-1}), $\Delta S^{\ddagger}_f$ (117 ± 4 J mol^{-1} K^{-1}), and $\Delta S^{\ddagger}_r$ (20 ± 6 J mol^{-1} K^{-1}) for the isomerization reaction. The $\Delta H^{\ddagger}_f$ is consistent with a proposed associative transition state involving partial cleavage of a Pd–P bond and partial formation of Pd–O(ether) bond to an adjacent ether oxygen. For comparison, *trans*-[$PtCl_2${$Ph_2P(CH_2CH_2O)_3CH_2CH_2PPh_2$-P,P′}] (*trans*-**2**) was isolated from a mixture of *cis* and *trans* isomers by column chromatography. An analysis of the isomerization process of *trans*-**2** to *cis*-**2** using quantitative $^{31}P\{^1H\}$ NMR spectroscopy revealed that no isomerization occurs at 348 K in the absence of an acid catalyst and that the acid-catalyzed *trans–cis* isomerization is zero order in complex. Crystal structures of *cis*-**1**, *cis*-**2**, and *trans*-**2** are also presented, and the conformations of the metallacrown ether rings in these structures have been related to the data presented above.

1. Introduction

Square planar transition metal complexes with phosphorus-donor ligands are important catalysts for a variety of organic reactions.[1] These complexes can exhibit both *cis* and *trans* geometrical isomers, and the isomer ratio can dramatically affect the activities and selectivities of the catalysis reactions. Thus, a large number of studies of these equilibria including measurements of the ΔH and ΔS have been carried out with the majority of these studies focusing on square planar Pt and Pd complexes containing either phosphane or phosphite ligands.[2–37]

Although a wealth of information has been obtained regarding the relative stabilities of the *cis* and *trans* isomers of the complexes,[38,39] very little information has been obtained regarding the kinetic parameters ($\Delta H^{\ddagger}_f$, $\Delta H^{\ddagger}_r$, $\Delta S^{\ddagger}_f$, and $\Delta S^{\ddagger}_r$) that would provide a better understanding of the reaction mechanisms. For Pd complexes, the primary reason for this is that the pure *cis* isomers of the complexes, which are needed for these studies, generally cannot be isolated. For Pt complexes, the pure *trans* isomers can be isolated, but they seem to be stable and do not isomerize.[1]

During our ongoing study of the coordination chemistry of metallacrown ethers, we have prepared the pure *cis*-$PdCl_2${$Ph_2P(CH_2CH_2O)_3CH_2CH_2PPh_2$-P,P′} (*cis*-**1**) and *trans*-$PtCl_2${$Ph_2P(CH_2CH_2O)_3CH_2CH_2PPh_2$-P,P′} (*trans*-**2**). The metallacrown ethers are excellent candidates for the study of the kinetics and thermodynamics of *cis–trans* isomerizations because the pure isomers can be isolated, they are stable in the solid state and they are quite soluble and the isomerizations occurs at rates that allow the reactions to be followed by $^{31}P\{^1H\}$ NMR spectroscopy. We have carried out these studies using quantitative $^{31}P\{^1H\}$ NMR spectroscopy, and the results are reported in this manuscript. We have also determined the X-ray crystal structures of both complexes and that of *cis*-**2** to gain additional insight into the factors that may be affecting the *cis–trans* isomerizations.

2. Results and Discussion

2.1 Synthesis and Characterization

We have previously demonstrated that the reaction of $Pd(PhCN)_2Cl_2$ and $Ph_2P(CH_2CH_2O)_3CH_2CH_2PPh_2$ (**1**) in dichloromethane yields an equilibrium mixture of *cis*- and *trans*-[$PdCl_2${$Ph_2P(CH_2CH_2O)_3CH_2CH_2PPh_2$-P,P′}]$_n$ mono-

[a] Department of Chemistry, University of Alabama at Birmingham,
901 14th Street South, Birmingham, Alabama 35294-1240, USA
Fax: +1-205-934-2543
E-mail: gmgray@uab.edu
[b] Avanti Polar Lipids, Inc.,
700 Industrial Park Drive, Alabaster, AL 35007, USA
[c] Department of Chemistry, Indiana University of Pennsylvania, Indiana, PA 15705, USA
Supporting information for this article is available on the WWW under http://www.eurjic.org or from the author.

mers (n = 1) and cyclic oligomers (n > 1).[38,40] In contrast, when this reaction is run in a 2:1 acetonitrile/THF mixture, the kinetic product *cis*-[$PdCl_2${$Ph_2P(CH_2CH_2O)_3CH_2CH_2$-$PPh_2$-P,P′}] (*cis*-**1**) precipitates from the reaction mixture.

We have also previously reported that the reaction of Pt(1,5-cod)Cl_2 and $Ph_2P(CH_2CH_2O)_3CH_2CH_2PPh_2$ under moderately high dilution conditions gives a high yield of *cis*-[$PtCl_2${$Ph_2P(CH_2CH_2O)_3CH_2CH_2PPh_2$-P,P′}] (*cis*-**2**)[41] In contrast, the reaction of $Ph_2P(CH_2CH_2O)_3CH_2CH_2PPh_2$ and $Pt(PhCN)_2Cl_2$ yields a mixture of *cis*- and *trans*-[$PtCl_2${$Ph_2P(CH_2CH_2O)_3CH_2CH_2PPh_2$-P,P′}] (*cis*-**2** and *trans*-**2**). The two isomers are easily separated via chromatography on silica gel using a 5:1 dichloromethane/ethyl acetate elutant with *cis*-**2** remaining at the origin and *trans*-**2** eluting from the column. The *trans* geometry of *trans*-**2** is indicated by the relatively small one-bond Pt–P coupling constant (2754 Hz).[25]

2.2 X-ray Crystal Structures of *cis*-1, *cis*-2 and *trans*-2

ORTEP diagrams showing the molecular structures of *cis*-**1**, *cis*-**2**, and *trans*-**2** are presented in Figures 1, 2, and 3, respectively. No anomalous intermolecular contacts were observed in these molecular structures. Selected bond lengths and angles for *cis*-**1**, *cis*-**2**, and *trans*-**2** are collected in Tables 1 and 2, respectively. The geometry associated with the primary coordination sphere about the metal center in each of the complexes is best described as a distorted square-planar geometry. The metallacrown ether ring is *cis*-chelated to the metal in *cis*-**1** and *cis*-**2** and *trans*-chelated to the metal in *trans*-**2**. The P1–M–P2 bond angles are 98.7(1)° in both the *cis* structures, *cis*-**1** and *cis*-**2**, suggesting that this distortion from square-planar geometry most likely results from the steric interactions between the adjacent diphenylphosphanyl groups. The average deviations from the least-squares plane (defined by the two phosphorus atoms, the two chlorides and the metal) for *cis*-**1**, *cis*-**2** and *trans*-**2** are 0.0502 Å, 0.01563 Å, and 0.0634 Å, respectively. This indicates that neither *cis* or *trans* chelation of the $Ph_2P(CH_2CH_2O)_3CH_2CH_2PPh_2$ ligand causes a significant out-of-plane distortion in the square-planar geometry.

The coordination geometry does have a significant effect on the metal–P and metal–Cl bond lengths. The metal–chloride bond lengths in *cis*-**1** and *cis*-**2** are significantly longer than are those in *trans*-**2**, while the metal–phosphane bonds in *cis*-**1** and *cis*-**2** are significantly shorter than are those in *trans*-**2**. These trends are consistent with the greater σ donor ability of a phosphane ligand relative to that of a chloride ligand.

The conformations of the metallacrown ether rings in *cis*-**1**, *cis*-**2** and *trans*-**2** are the most interesting aspects of the structures. Values of selected torsion angles for *cis*-**1**, *cis*-**2** and *trans*-**2**, given in Table 3, indicate that the three metallacrown ethers have rather different ring conformations. One similarity between the structures is that the torsion angles around the ethylene groups (defined by O–C–C–O) are all pseudo-*gauche*. This is consistent with the tendency of such groups to orient in a *cis* conformation and has previously been observed in the X-ray crystal structures of related metallacrown ether complexes.[42–46]

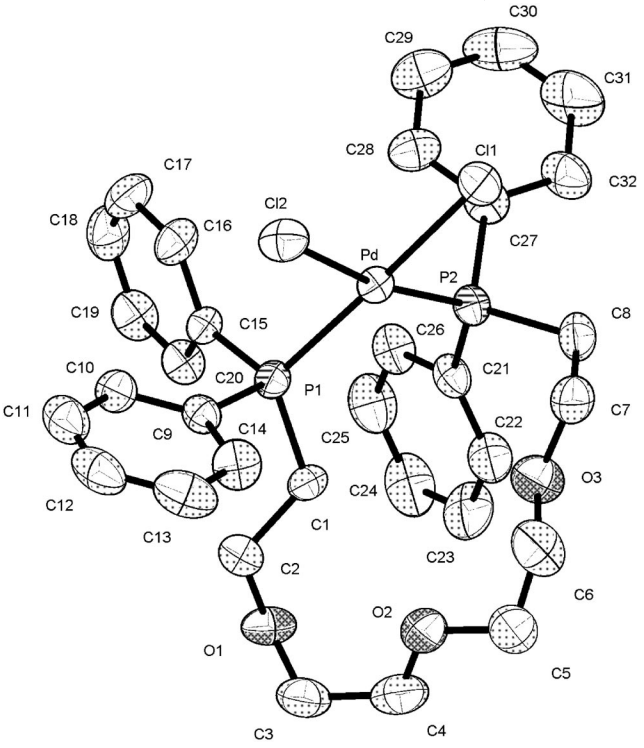

Figure 1. ORTEP drawing of the molecular structure of *cis*-**1**. Thermal ellipsoids are drawn at the 50% probability level, and hydrogen atoms are omitted for clarity.

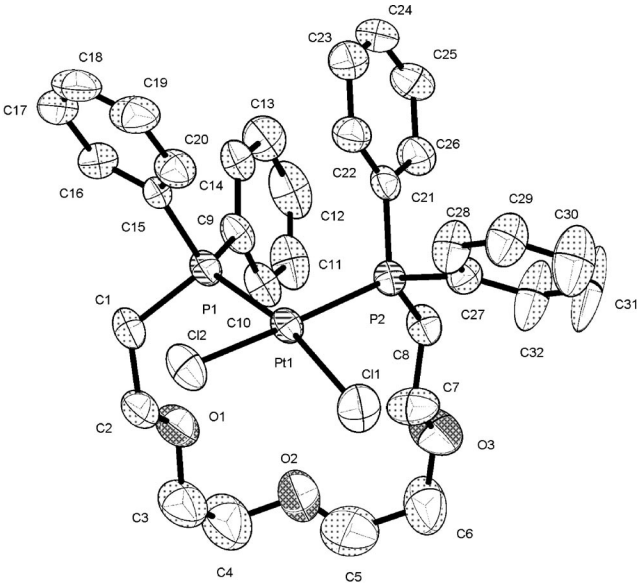

Figure 2. ORTEP drawing of the molecular structure of *cis*-**2**. Thermal ellipsoids are drawn at the 50% probability level, and hydrogen atoms are omitted for clarity.

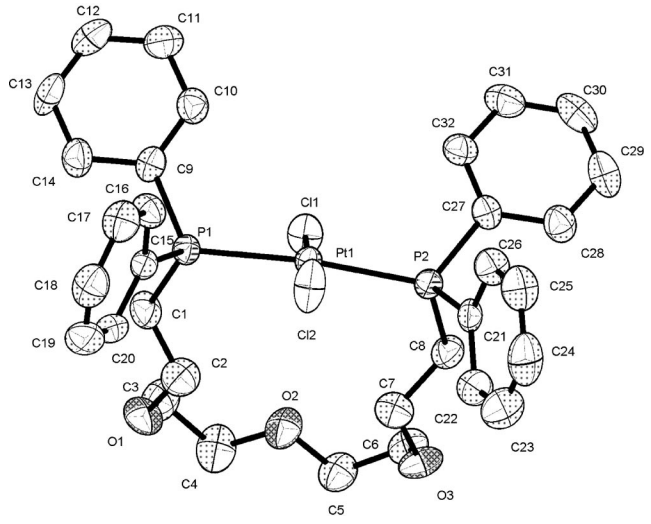

Figure 3. ORTEP drawing of the molecular structure of *trans*-**2**. Thermal ellipsoids are drawn at the 50% probability level, and hydrogen atoms are omitted for clarity.

Table 1. Selected bond lengths [Å] for *cis*-**1**, *cis*-**2**, and *trans*-**2**.

	cis-**1**	*cis*-**2**	*trans*-**2**
About metal			
M–Cl2	2.3425(15)	2.3526(19)	2.2838(13)
M–Cl1	2.3595(15)	2.339(2)	2.3098(13)
M–P1	2.2568(16)	2.2476(19)	2.3118(14)
M–P2	2.2763(15)	2.2447(19)	2.3143(14)
About P			
P1–C1	1.821(5)	1.838(7)	1.824(5)
P1–C15	1.815(5)	1.821(7)	1.817(5)
P1–C9	1.826(5)	1.816(7)	1.817(5)
P2–C8	1.827(6)	1.803(7)	1.834(5)
P2–C21	1.834(5)	1.805(7)	1.819(5)
P2–C27	1.821(6)	1.826(7)	1.828(5)
Around ring			
C1–C2	1.518(7)	1.494(10)	1.453(7)
C2–O1	1.418(7)	1.369(9)	1.441(6)
O1–C3	1.418(7)	1.445(11)	1.398(7)
C3–C4	1.495(9)	1.403(13)	1.500(8)
C4–O2	1.411(7)	1.411(13)	1.423(7)
O2–C5	1.401(7)	1.276(15)	1.407(6)
C5–C6	1.485(10)	1.473(16)	1.494(8)
C6–O3	1.404(7)	1.391(12)	1.405(6)
O3–C7	1.416(7)	1.407(9)	1.439(6)
C7–C8	1.526(8)	1.500(10)	1.498(7)

Table 2. Selected bond angles [°] for *cis*-**1**, *cis*-**2**, and *trans*-**2**.

	cis-**1**	*cis*-**2**	*trans*-**2**
About metal			
P1–M–P2	98.68(6)	98.76(6)	173.01(4)
Cl1–M–Cl2	88.91(6)	87.79(8)	178.99(5)
Cl1–M–P1	177.75(6)	167.53(8)	87.50(5)
Cl1–M–P2	83.53(6)	88.41(7)	89.88(5)
Cl2–M–P2	170.71(6)	170.38(7)	91.13(5)
Cl2–M–P1	88.85(6)	86.61(7)	91.50(5)
About P			
M–P1–C1	117.86(19)	111.8(2)	111.25(18)
M–P1–C9	113.10(18)	117.8(2)	116.34(16)
M–P1–C15	108.23(18)	115.1(2)	115.07(16)
C1–P1–C9	102.5(2)	103.5(3)	102.0(2)
C1–P1–C15	107.6(3)	101.1(3)	107.8(2)
C9–P1–C15	106.9(3)	105.7(3)	103.2(2)
M–P2–C8	110.0(2)	114.7(2)	111.83(17)
M–P2–C21	124.16(18)	115.9(2)	114.91(16)
M–P2–C27	107.51(19)	112.9(2)	118.01(17)
C8–P2–C21	106.5(3)	104.8(3)	105.6(2)
C8–P2–C27	106.7(3)	106.7(3)	100.8(2)
C21–P2–C27	100.5(3)	100.3(3)	104.0(2)
Around ring			
P1–C1–C2	115.7(4)	121.2(5)	118.8(4)
C1–C2–O1	110.5(5)	112.5(7)	111.3(5)
C2–O1–C3	115.4(5)	110.3(7)	117.1(4)
O1–C3–C4	113.7(5)	111.6(9)	113.7(5)
C3–C4–O2	111.0(6)	116.1(11)	109.2(5)
C4–O2–C5	113.7(6)	121.4(13)	111.8(4)
O2–C5–C6	111.2(6)	120.0(15)	109.8(5)
C5–C6–O3	108.8(6)	115.3(9)	114.4(5)
C6–O3–C7	115.3(5)	115.4(8)	114.7(4)
O3–C7–C8	108.5(5)	106.3(6)	110.1(4)
C7–C8–P2	114.1(4)	114.9(5)	117.6(4)

Table 3. Selected torsion angles [°] for *cis*-**1**, *cis*-**2**, and *trans*-**2**.

	cis-**1**	*cis*-**2**	*trans*-**2**
M–P1–C1–C2	159.2(4)	–32.4(7)	30.5(5)
P1–C1–C2–O1	168.7(4)	–72.8(8)	–176.8(4)
C1–C2–O1–C3	102.0(6)	–177.4(7)	86.5(6)
C2–O1–C3–C4	–93.0(7)	–174.2(9)	93.6(6)
O1–C3–C4–O2	72.9(7)	59.2(15)	–75.9(7)
C3–C4–O2–C5	175.0(6)	86.1(17)	179.4(5)
C4–O2–C5–C6	164.6(6)	175.3(11)	177.3(5)
O2–C5–C6–O3	–73.8(8)	47(2)	74.4(6)
C5–C6–O3–C7	–171.2(6)	60.2(15)	–87.3(6)
C6–O3–C7–C8	172.8(5)	–176.2(8)	–85.4(6)
O3–C7–C8–P2	65.3(6)	174.0(6)	–174.4(3)
C7–C8–P2–M	40.0(5)	–35.8(7)	–34.0(5)
C8–P2–M–P1	–123.7(2)	–84.4(3)	11.8(4)
P2–M–P1–C1	39.1(2)	141.5(3)	–11.1(4)

The oxygen–oxygen distances for *cis*-**1**, *cis*-**2** and *trans*-**2** and for the related metallacrown ethers, *cis*-[$Mo(CO)_4$-{$Ph_2P(CH_2CH_2O)_3CH_2CH_2PPh_2$-P,P′}], *cis*-**4**, and *trans*-[$Mo(CO)_4Ph_2P(CH_2CH_2O)_3CH_2CH_2PPh_2$-P,P′}], *trans*-**4**, (Table 4) allow the cavity sizes in the various metallacrown ether rings to be compared. The distances between adjacent oxygens (O3···O6 and O6···O9) in all of the complexes range from 2.842 to 3.052 Å and are on average 2.942 Å. These distances are consistent with pseudo-gauche configurations about the O–C–C–O groups. The distances between nonadjacent oxygens strongly depend on the coordination geometry at the metal center.[42–46] As expected, the complexes with *cis*-chelated phosphanes (*cis*-**1**, *cis*-**2**, *cis*-**4**) have shorter O3···O9 distances than do the complexes with *trans*-chelated phosphane (*trans*-**2**, *trans*-**4**). The differences in the O3···O9 distances reflect the larger chelate bite angles of the *trans*-chelated bis(phosphane)-polyether ligands. The fact that this distance is larger in *trans*-**4** than in *trans*-**2** is most likely a result of the steric interactions between axial CO ligands with the metallacrown ring in *trans*-**4**.

Table 4. Oxygen–oxygen distances in *cis*-**1**, *cis*-**2**, *trans*-**2**, *cis*-**4**, and *trans*-**4**.

	O1···O3 [Å]	O1···O2 [Å]	O2···O3 [Å]
cis-**1**	5.067	3.003	2.911
cis-**2**	4.766	2.863	2.865
trans-**2**	5.309	3.001	2.997
cis-**4**	4.480	2.842	2.883
trans-**4**	5.527	3.052	3.031

The relative orientations of the metallacrown ether ring, as defined by the plane containing the ether oxygens, and the metal complex, as defined by the least-squares plane of the metal and the two phosphorus atoms, are also of interest. For the complexes with *cis*-chelated phosphanes (*cis*-**1**, *cis*-**2**, *cis*-**4**), the dihedral angles between these planes are 95.5°, 94.6°, and 95.1°, respectively. The similar angles suggest that there is little interaction between the metallacrown ether ring and the metal center in the *cis*-metallacrown ethers. In contrast, the dihedral angles between the two planes in the *trans*-metallacrown ethers, *trans*-**2** (3.6°) and *trans*-**4** (68.0°), are very different. This difference is most likely due to the fact that the metallacrown ether ring in a complex with *trans*-chelated phosphanes wraps around the metal centers, and thus their orientations are strongly influenced by the nature of the metal center.

2.3 Thermodynamics of the *cis–trans* Isomerization of *cis*-1

The *cis–trans* equilibrium constants were calculated at four temperatures from the equilibrium concentrations of monomeric *cis*-**1** and of both monomeric and oligomeric *trans*-**1** and are given in Table 5. The *cis–trans* equilibrium constants increase with increasing temperature.

Table 5. Equilibrium constants for the *cis–trans* equilibrium in **1** at various temperatures.

Temp. [K]	Integration *cis*-**1**	Integration *trans*-**1**	[*cis*-**1**] (M)	[*trans*-**2**] (M)	*K*
326	1.00	0.323	0.0677	0.0219	0.323
341	1.00	0.560	0.0574	0.0322	0.560
348	1.00	0.713	0.0523	0.0373	0.713
356	1.00	0.983	0.0452	0.0444	0.983
392	1.00	2.93	0.0228	0.0668	2.93
422	1.00	6.42	0.0121	0.0775	6.42

A plot of $-R\ln K$ vs. $1/T$ is linear over the temperature range, as shown in Figure 4, and gives both the enthalpy (ΔH) and entropy (ΔS) changes for the *cis–trans* equilibrium of **1** ($\Delta H = +35.8 \pm 0.2$ kJ/mol; $\Delta S = +100.2 \pm 0.8$ J/mol K). These values are similar to those previously reported by Verstuyft and Nelson for *cis–trans* equilibria of $Pd\{p\text{-}XC_6H_4)_2PMe\}_2Cl_2$ (X = Cl, H, Me) complexes in the same solvent (ΔH = +14.6, 26.8 and 33.9 kJ/mol; ΔS = +44.4, 79.1 and 103.8 J/mol K, respectively).[27] As was previously suggested by Verstuyft and Nelson, the positive ΔH indicates that stronger bonding occurs in the *cis* isomer in which the Cl^- ligands are opposite to the phosphanes and the positive ΔS suggests that the *cis* isomer is more ordered due to crowding. Such crowding is observed in the X-ray crystal structures of *cis*-**2**, discussed above, and of *cis*-**4**,[42] where the $Ph_2P(CH_2CH_2O)_3CH_2CH_2PPh_2$ ligand is packed only in one quadrant of the complex. In contrast, in the X-ray crystal structures of *trans*-**2**, discussed above, and of *trans*-**4**,[47] the $Ph_2P(CH_2CH_2O)_3CH_2CH_2PPh_2$ ligand is spread out to cover a hemisphere of the complex. Crowding in *cis*-metallacrown ethers has also been used to explain the unexpected conformation equilibria in solutions of *cis*-$Mo(CO)_4\{Ph_2P(CH_2CH_2O)_5CH_2CH_2PPh_2\}$ and of *cis*-$PtCl_2\{Ph_2P(CH_2CH_2O)_5CH_2CH_2PPh_2\}$ metallacrown ethers.[47]

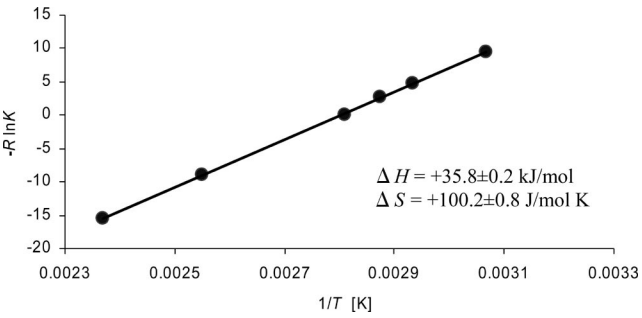

Figure 4. Plot of $-R\ln K$ vs. $1/T$ for the *cis–trans* isomerization of *cis*-**1**.

2.4 Kinetics of the *cis–trans* Isomerization of *cis*-1

The kinetic parameters for the forward and reverse reactions of the *cis–trans* isomerization of *cis*-**1**, have been determined using an Eyring analysis. The conversion of *cis*-**1** to *trans*-**1** at four temperatures (331, 341, 348, and 356 K) was followed with $^{31}P\{^1H\}$ NMR spectroscopy. As shown in Figure 5, although the concentration of the solution was low, a small amount of the oligomeric *trans*-**1** was still formed. The concentration of *cis*-**1** and *trans*-**1** were determined from the integrations of the resonances at δ = 27 ppm (monomeric *cis*-**1**), 16 ppm (monomeric *trans*-**1**) and 15 ppm (oligomeric *trans*-**2**) and the initial concentration of the *cis*-**1**. The reversible first-order rate constants for the forward reactions at each of the temperatures were extracted from plots of $-\ln(1\text{-}[\textit{trans}\text{-}\mathbf{1}]/[\textit{trans}\text{-}\mathbf{1}]_e)$ vs. time. A plot of this type for the 331 K data is shown in Figure 6. The reversible first-order rate constants for the reverse reactions were calculated from the reversible first-order rate constants for the forward reactions and the equilibrium constants.

The kinetic parameters for the activation process were determined from plots of the type shown in Figure 7. The ΔH and ΔS for the equilibrium determined from these kinetic parameters ($\Delta H = \Delta H^{\ddagger}_f - \Delta H^{\ddagger}_r = +36 \pm 3$ kJ/mol; $\Delta S = \Delta S^{\ddagger}_f - \Delta S^{\ddagger}_r = +98 \pm 7$ J/mol K) are in excellent agreement with the ΔH and ΔS obtained from the data reported in Table 5 ($\Delta H = +35.8 \pm 0.2$ kJ/mol; $\Delta S = +100.2 \pm 0.8$ J/mol K).

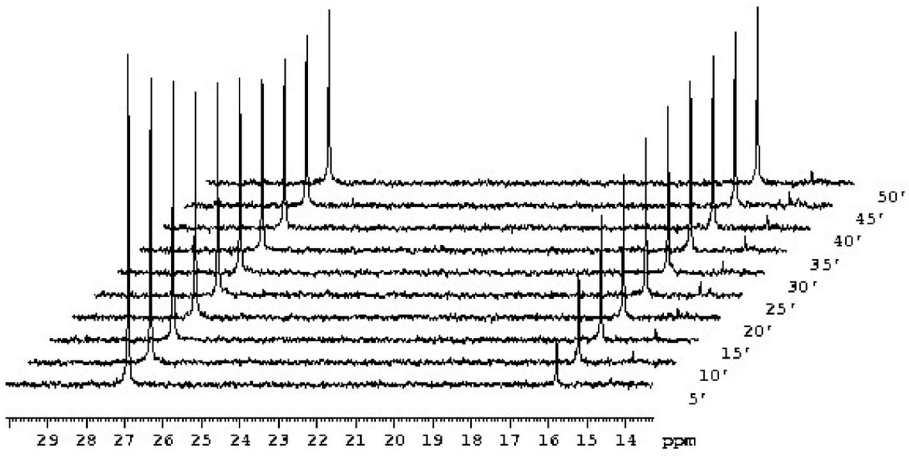

Figure 5. $^{31}P\{^{1}H\}$ NMR spectra of the isomerization of *cis*-**1** to *trans*-**1** at 331 K.

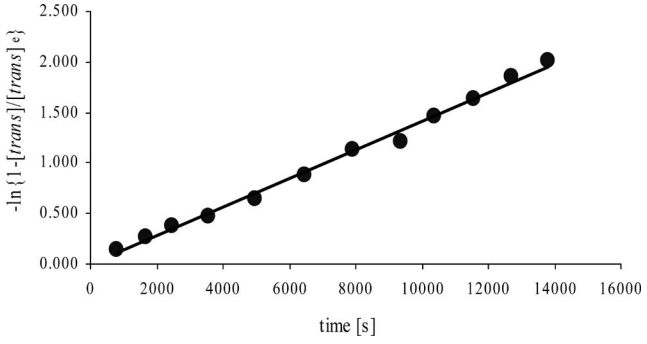

Figure 6. Reversible first order kinetics plot of the conversion of *cis*-**1** to *trans*-**1** at 331 K.

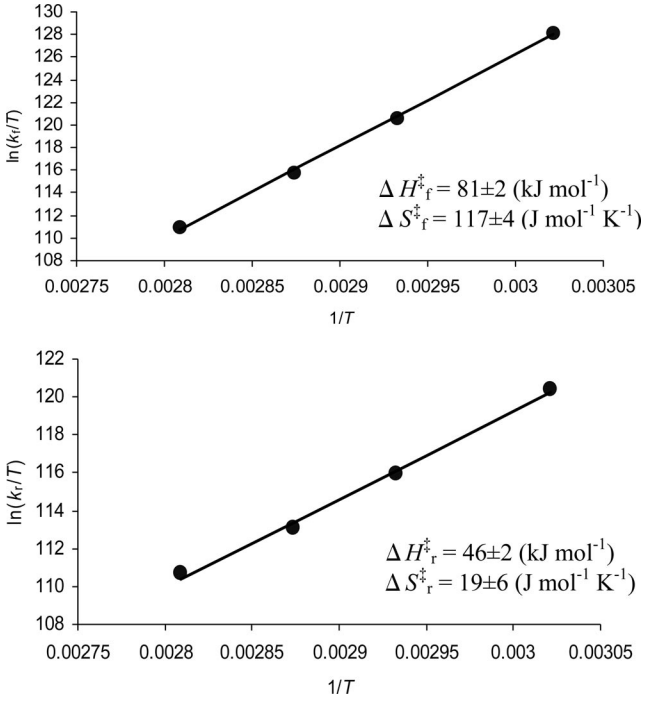

Figure 7. Results from an Eyring analysis of the *cis–trans* isomerization of *cis*-**1**.

2.5 Mechanism of *cis–trans* and Monomer–Oligomer Equilibria of *cis*-1

The most interesting observation of our previous studies of the *simultaneous cis–trans* and monomer–oligomer equilibria of *cis*-$PdCl_2\{Ph_2P(CH_2CH_2O)_nCH_2CH_2PPh_2$-P,P′} ($n$ = 3 (*cis*-**1**), 4, 5) metallacrown ethers was that the dimerization and oligomerization equilibrium constants of the metallacrown ethers were much smaller than were those for *cis*-$PdCl_2\{Ph_2P(CH_2)_{12}PPh_2$-P,P′} even though the chelate rings sizes in the three metallacrown ethers bracketed those in the bis(phosphane) complex.[39,40] The dimerization and oligomerization reactions for any complex require that a phosphane dissociate from a palladium and then attack another palladium to form the next higher oligomer (oligomerization). This attack could form either *cis* or *trans* centers in the oligomer. If the dissociated phosphane instead recombines with the original palladium, this can either regenerate the monomeric *cis* complex (recombination) or form a monomeric *trans* complex (isomerization).

Although the dimerization and oligomerization reactions must involve cleavage of a Pd–P bond, other mechanisms are possible for the isomerization reaction. However, during the studies of the *cis–trans* isomerization of *cis*-**1** that are reported in this paper, we observed that *cis*-**1** *simultaneously* converts to a mixture of *trans*-**1** and cyclic oligomers of *trans*-**1** at higher concentrations and that this conversion still obeys reversible first order kinetics. This behavior suggests that the rate-determining step for both the *cis–trans* and monomer–oligomer equilibria is the same and thus must involve cleavage of a Pd–P bond.

The large differences in the equilibrium constants for the dimerization and oligomerization reactions for the *cis*-$PdCl_2\{Ph_2P(CH_2CH_2O)_nCH_2CH_2PPh_2$-P,P′} ($n$ = 3 (*cis*-**1**), 4, 5) and *cis*-$PdCl_2\{Ph_2P(CH_2)_{12}PPh_2$-P,P′} complexes cannot be due to differences in the palladium-phosphane bond strengths because the phosphanes are nearly identical in the four complexes. Instead, the differences in the equilibrium constants must be due to differences in the relative rates of the recombination, isomerization and oligomerization reac-

tions. These reactions would be expected to proceed by an associative mechanism because the complexes are 16 valence electron square-planar complexes.[48] In the metallacrown ether complexes, the transition state might be expected to involve partial dissociation of the palladium-phosphane bond and partial formation of a palladium–oxygen bond to an adjacent ether oxygen. The hemilabile coordination of one of the ether oxygens to the palladium would keep the free phosphane relatively close to the palladium, favoring recombination and isomerization over oligomerization. In contrast, in the bis(phosphane) complex, this hemilabile oxygen coordination could not occur, and the recombination reactions would be less favored.

If the transition state for both reactions involves partial dissociation of the palladium-phosphane bond and partial formation of a palladium–oxygen bond, the $\Delta H^{\ddagger}_{f}$ value should be significantly less than the bond dissociation energy for a palladium-phosphane bond. There is little data available in the literature for the strengths of Pd–P bonds[49–53] and none for Pd–O(ether) bonds; however, one study has reported a "ligand bonding power" of 162 kJ mol^{-1} for the Pd–PEt_3 bonds in *cis*-[$Pd(PEt_3)_2Cl_2$] complex based on microcalorimetry data,[53] and several computational studies performed on these types of systems[49,52] have given similar calculated bond strengths. The fact that the $\Delta H^{\ddagger}_{f}$ for *cis*-**1** (81 ± 2 kJ mol^{-1}) is significantly less than the "ligand bonding power" of 162 kJ mol^{-1} is consistent with the proposed transition state.

The fact that the $\Delta H^{\ddagger}_{f}$ for *cis*-**1** is less that the "ligand bonding power" cannot be explained by solvation effects. If solvation is important, the decrease in solvation in the polar 1,2-[D_2]tetrachloroethane upon isomerization should result in $\Delta H^{\ddagger}_{f}$ for *cis*-**1** being larger than the "ligand bonding power" because *cis*-**1** is more polar than is *trans*-**1**.

2.6 Kinetics of the *trans–cis* Isomerization of *trans*-2

As mentioned in the Introduction, *trans*-Pt(phosphane)$_2$-Cl_2 complexes, unlike *cis*-Pd(phosphane)$_2Cl_2$ complexes, can be isolated and purified without isomerization occurring. To gain insight into the mechanisms of the isomerization reactions of the two types of complexes, we have studied the kinetics of the *trans–cis* isomerization of **2** using $^{31}P\{^1H\}$ NMR spectroscopy. No isomerization occurred in pure 1,2-[D_2]tetrachloroethane at 348 K, however, upon addition of a drop of a 12 M solution of DCl in D_2O to a solution of *trans*-**2** in 1,2-[D_2]tetrachloroethane, isomerization of the complex is observed. The relative amounts of each isomer were measured as a function of the integrals of *trans* peaks located at δ = 13 ppm and the *cis* peaks located at 7 ppm. The time-resolved $^{31}P\{^1H\}$ NMR of *trans*-[$PtCl_2\{Ph_2P(CH_2CH_2O)_3CH_2CH_2PPh_2$-P,P′}] in 1,2-[$D_2$]-tetrachloroethane at 348 K are shown in Figure 8. Analysis of this data showed that the acid-catalyzed isomerization of **2** followed zero-order kinetics and exhibited an excellent fit to a plot of [*trans*-**2**] vs. time. (Figure 9).

The fact that the isomerization of *trans*-**2** does not occur at an observable rate at 348 K in 1,2-[D_2]tetrachloroethane in the absence of an acid catalyst is consistent with our earlier observations that the reactions of $PtCl_2$(cod) and $Ph_2P(CH_2CH_2O)_nCH_2CH_2PPh_2$ (n = 3, 4, 5) yield only the monomeric *cis* metallacrown ethers. Based on the above studies with *cis*-**1**, the kinetic product of the reactions would be expected to be the *cis*-$PtCl_2\{Ph_2P(CH_2CH_2O)_n$-$CH_2CH_2PPh_2$-P,P′} ($n$ = 3, 4, 5) metallacrown ethers, and these complexes should neither isomerize nor oligomerize at ambient reaction temperature.

Although the isomerization of *trans*-**2** does not occur in 1,2-[D_2]tetrachloroethane at 348 K in the absence of acid,

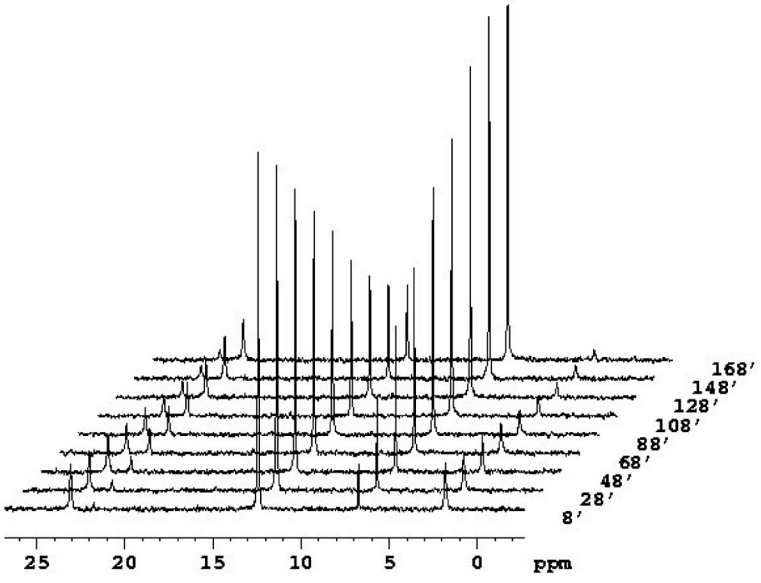

Figure 8. $^{31}P\{^1H\}$ NMR spectra of the isomerization of *trans*-**2** to *cis*-**2**.

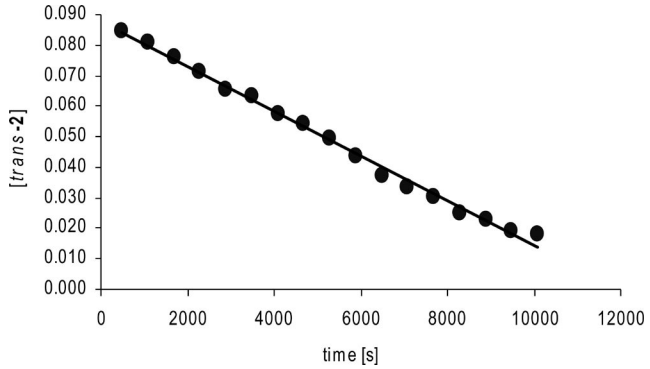

Figure 9. Plot of the concentration of [*trans*-**2**] vs. time for the *trans–cis* isomerization of *trans*-**2** showing that the isomerization is zero order in *trans*-**2**.

it does occur in [D]chloroform at the same temperature. The most likely explanation is that the chloroform contains a small amount of acid and not that the mechanism is different in the two solvents.

3. Conclusions

The *cis–trans* isomerization equilibrium of the palladium(II) metallacrown ether *cis*-**1** follows reversible first-order kinetics, and both the thermodynamic and kinetic parameters for this reaction have been determined. These parameters, when analyzed in light of results from studies of monomer–oligomer equilibria and the X-ray crystal structures of *cis*-**1**, *cis*-**2**, and *trans*-**2**, suggest that the transition state involves cleavage of a Pd–P bond and formation of Pd–O(ether) bond to an adjacent ether oxygen. In contrast, the *trans–cis* isomerization of platinum(II) metallacrown ether *trans*-**2** to *cis*-**2** does not occur in the absence of an acid catalyst, and the acid catalyzed *trans–cis* isomerization is zero order in complex. These studies clearly demonstrate that palladium(II) and platinum(II) complexes with identical ligands and coordination geometries can exhibit very different reaction mechanisms for the same reactions under identical reaction conditions. If this is a general trend, it could help to explain why similar palladium(II) and platinum(II) complexes can exhibit very different catalytic activities and selectivities for the same reactions.

4. Experimental Section

4.1 General Procedures

Multinuclear $^{31}P\{^1H\}$, $^{13}C\{^1H\}$, and ^1H NMR spectra were recorded on a Bruker ARX300 FT-NMR variable temperature spectrometer. All downfield chemical shifts are reported as positive. The ^1H NMR and $^{13}C\{^1H\}$ chemical shifts were referenced either to tetramethylsiliane or [D]chloroform (δ =77.23 ppm). The $^{31}P\{^1H\}$ chemical shifts were referenced to external 85% phosphoric acid (capillary) in [D]chloroform. Atlantic Microlabs of Norcross, GA performed all elemental analyses. Quantitative $^{31}P\{^1H\}$ NMR spectra were obtained using an inverse gate pulse sequence with an 30° pulse and a delay of 20 s. This method was tested on mixtures of *cis*-$Mo(CO)_4$(phosphane)$_2$ complexes and the $^{31}P\{^1H\}$ NMR integrations of the $^{31}P\{^1H\}$ NMR resonances were observed to be proportional to the molarities of the complexes in the solutions. The starting materials: $Ph_2P(CH_2CH_2O)_3CH_2CH_2PPh_2$[40] and $Pt(PhCN)_2Cl_2$[54,55] and the *cis*-[$PtCl_2\{Ph_2P(CH_2CH_2O)_3CH_2CH_2$-$PPh_2$-P,P′}] (*cis*-**2**) metallacrown ether[41] were prepared using literature procedures.

***cis*-[$PdCl_2\{Ph_2P(CH_2CH_2O)_3CH_2CH_2PPh_2$-P,P′}] (*cis*-1):** A mixture of 0.434 g (2.45 mmol) of palladium(II) chloride and 1.30 g (2.45 mmol) of $Ph_2P(CH_2CH_2O)_3CH_2CH_2PPh_2$ was dissolved in 25 mL of a 2:1 acetonitrile/tetrahydrofuran mixture at ambient temperature. After stirring overnight, a pale yellow precipitate had formed. The solid was collected, washed with acetonitrile (3 × 50 mL) and dried in vacuo (0.02 Torr at 298 K) for 48 h yielding 1.21 g (69.8%) of *cis*-**1**. The filtrate was evaporated to dryness (21 Torr at 315 K), and the orange oily residue was purified by column chromatography on silica gel with ethyl acetate as the eluant (R_f = 0.35) to yield 0.450 g (26.0%) of an equilibrium mixture of **1**. ^1H NMR of *cis*-**1** ([D]chloroform, 300 MHz): δ = 2.18–2.92 (m, 4 H, P-CH_2) 3.42–4.23 (m, 12 H, O-CH_2), 7.79–7.09 (m, 20 H, C_6H_5-P). $^{31}P\{^1H\}$ NMR of *cis*-**1** ([D]chloroform, 121.5 MHz): δ = 24.37 (s) ppm. $C_{32}H_{36}Cl_2O_3P_2Pd$ (706.05): calcd. C 54.32, H 5.08, Cl 10.02; found C 54.18, H 5.19, Cl 9.94.

***trans*-[$PtCl_2\{Ph_2P(CH_2CH_2O)_3CH_2CH_2PPh_2$-P,P′}] (*trans*-2):** A solution of 0.723 g (1.36 mmol) of $Ph_2P(CH_2CH_2O)_3CH_2CH_2PPh_2$ in 125 mL of dichloromethane was slowly added to a solution of 0.644 g (1.36 mmol) of $Pt(PhCN)_2Cl_2$ in 400 mL of dichloromethane, and the resulting solution was stirred at ambient temperature for 20 h. Then, the solution was reduced in volume to 10 mL, and the concentrate was poured into 500 mL of hexanes. The pale yellow precipitate was collected by filtration, washed with hexanes (3 × 30 mL) and dried in vacuo (0.02 Torr at 298 K) for 48 h to yield 0.868 g (80.1%) of a mixture of *cis*-**2** and *trans*-**2**. Chromatography on silica with 5:1 dichloromethane/ethyl acetate mixture (R_f = 0.45) yielded *trans*-**2**. Recrystallization from a hexanes and dichloromethane solution yielded 0.431 grams (39.8%) of analytically pure *trans*-**2**. $C_{32}H_{36}Cl_2O_3P_2Pt$ (795.11): calcd. C 48.25, H 4.55, Cl 8.90; found C 48.18, H 4.60, Cl 8.99. ^1H NMR ([D]chloroform, 300 MHz): δ = 2.18–2.92 (m, 4 H, PCH_2), 3.42–4.53 (m, 12 H, OCH_2), 7.79–7.09 (m, 20 H, C_6H_5P) ppm. $^{31}P\{^1H\}$ NMR ([D] chloroform, 121.5 MHz): δ = 11.03, (s&d, $|^1J$(Pt-P)| = 2574 Hz) ppm.

4.2 Collection, Solution and Refinement of X-ray Diffraction Data

All crystals in this study were grown by slow evaporation of their dichloromethane/hexanes solutions. Suitable X-ray quality single crystals of each compound were individually sealed into thin-walled glass capillaries under aerobic conditions. Each crystal was then mounted and aligned upon an Enraf–Nonius CAD4 single crystal diffractometer with κ-geometry (graphite monochromated Mo-K_α radiation, λ = 0.71073 Å). Details of the data collections are collected in Table 6. All data were corrected for Lorentz and polarization effects.

The lattice parameters and the systematic absences of *cis*-**1** and *trans*-**2** (*h0l* for $h + l = 2n + 1$ and *0k0* for $k = 2n + 1$) uniquely defined the space group of both these crystals as $P2_1/n$ (No. 14). The lattice parameters and systematic absences of *cis*-**2** (*hkl* for $h + k = 2n + 1$ and *h0l* for $l = 2n + 1$) were consistent with either the centrosymmetric space group $C2/c$ (No. 15) or the noncentrosymmetric space group *Cc* (No. 9). Intensity statistics favored the centrosymmetric choice of $C2/c$. The successful solution and refinement of the crystal structure later verified this.

Table 6. Crystal and structure refinement data for *cis*-**1**, *cis*-**2**, and *trans*-**2**.

	cis-**1**	*cis*-**2**	*trans*-**2**
Empirical formula	$C_{32}H_{36}Cl_2O_3P_2Pd$	$C_{32}H_{36}Cl_2O_3P_2Pt$	$C_{32}H_{36}Cl_2O_3P_2Pt$
CCDC deposit no.	661698	661700	661699
Formula weight	707.85	796.54	796.54
Temperature	293(2) K	293(2) K	293(2) K
Wavelength	0.71073 Å	0.71073 Å	0.71073 Å
Crystal system		monoclinic	
Space group	$P2_1/n$	$C2/c$	$P2_1/n$
Unit cell dimensions	a = 11.780(2) Å	a = 28.277(6) Å	a = 16.496(3) Å
	b = 16.159(3) Å	b = 11.603(2) Å	b = 10.080(2) Å
	c = 16.911(3) Å	c = 21.706(4) Å	c = 19.789(4) Å
	α = 90°	α = 90°	α = 90°
	β = 101.23(3)°	β = 109.08(3)°	β = 109.79(3)°
	γ = 90°	γ = 90°	γ = 90°
Volume	3157.3(11) Å^3	6730(2) Å^3	3096.4(11) Å^3
Z	4	8	4
Density (calculated)	1.489 Mg/m^3	1.572 Mg/m^3	1.709 Mg/m^3
Absorption coefficient	0.890 [mm]$^{-1}$	4.453 mm^{-1}	4.840 mm^{-1}
F(000)	1448	3152	1576
Crystal size	0.2 × 0.2 × 0.15 mm^3	0.25 × 0.2 × 0.1 mm^3	0.25 × 0.2 × 0.2 mm^3
Theta range for data collection	2.17 to 22.48°	1.52 to 22.47°	2.19 to 22.50°
Index ranges	$0 \le h \le 12$, $0 \le k \le 17$, $-18 \le l \le 17$	$-20 \le h \le 30$, $-8 \le k \le 12$, $-23 \le l \le 22$	$0 \le h \le 17$, $-10 \le k \le 10$, $-21 \le l \le 20$
Reflections collected	4348	5626	8111
Independent reflections	4116 [R(int) = 0.0410]	4389 [R(int) = 0.0533]	4034 [R(int) = 0.0306]
Completeness to θ = 22.48°	99.7%	100.0%	99.8%
Absorption correction		none	
Refinement method		full-matrix least-squares on F^2	
Data/restraints/parameters	4116/0/362	4389/0/362	4034/0/362
Goodness-of-fit on F^2	0.995	0.982	1.071
Final R indices [$I > 2\sigma(I)$]	R_1 = 0.0337, $wR2$ = 0.0759	R_1 = 0.0321, $wR2$ = 0.0783	R_1 = 0.0231, $wR2$ = 0.0565
R indices (all data)	R_1 = 0.0834, $wR2$ = 0.0901	R_1 = 0.0555, $wR2$ = 0.0839	R_1 = 0.0327, $wR2$ = 0.0591

All crystallographic calculations were performed with the Siemens SHELXTL-PC program package.[56] Heavy atoms were located using a Patterson method and the remaining atoms were located from difference Fourier analysis. All hydrogen atoms were placed in calculated positions with the appropriate molecular geometry and a δ(C–H) = 0.96 Å. The isotropic thermal parameter associated with each hydrogen atom was fixed equal to the U_{eq} of the carbon atom to which it was bound. The positional and anisotropic thermal parameters for all non-hydrogen atoms were refined. The tool SQUEEZE, from PLATON,[57,58] was used to calculate the number of electrons of disordered solvent for the one void in *trans*-**2**. The total number of electrons was determined to be 42.1, which equates to approximately one molecule of dichloromethane.

CCDC-661698 (for *cis*-**1**), -661700 (for *cis*-**2**), and -661699 (for *trans*-**2**) contain the supplementary crystallographic data for this paper. These data can be obtained free of charge from The Cambridge Crystallographic Data Centre via www.ccdc.cam.ac.uk/data_request/cif.).

4.3 ^{31}P NMR Studies of the Isomerization Reactions of the Metallacrown Ethers

Equilibrium Constants: Equilibrium constants for the *cis–trans* isomerizations of *cis*-**1** were measured at four temperatures. At each temperature, a 5 mm, screw-capped NMR tube containing 0.042 g (0.058 mmol) of *cis*-**1** dissolved in 0.60 mL of 1,2-[D_2]tetrachloroethane was allowed to stand until no change in the ratio of *cis*-**1** to *trans*-**1** was observed (at least 18 h). The equilibrium concentrations of *cis*-**1** and *trans*-**1** were calculated from the integrals of the ^{31}P{^{1}H} NMR resonances of monomeric *cis*-**1** at δ = 27 ppm (I_{cis}), monomeric *trans*-**1** at δ = 16 ppm ($I_{trans\ mono}$) and oligomeric *trans*-**1** at δ = 15 ppm ($I_{trans\ oligo}$) and the initial concentration of *cis*-**1** ([*cis*-1]$_i$) using Equations (1) and (2).

$$[cis\text{-}\mathbf{1}] = \frac{I_{cis}}{I_{cis} + I_{trans\ mono} + I_{trans\ oligo}} [cis\text{-}\mathbf{1}]_i \quad (1)$$

$$[trans\text{-}\mathbf{1}] = \frac{I_{trans\ mono} + I_{trans\ oligo}}{I_{cis} + I_{trans\ mono} + I_{trans\ oligo}} [cis\text{-}\mathbf{1}]_i \quad (2)$$

The *cis–trans* equilibrium constants were calculated from the equilibrium concentrations using Equation (3) and are given in Table 5. The *cis–trans* equilibrium constants increase with increasing temperature.

$$K = \frac{[trans\text{-}\mathbf{1}]_e}{[cis\text{-}\mathbf{1}]_e} \quad (3)$$

Rate Constants: Rate constants for the *cis–trans* isomerizations of *cis*-**1** were also measured at four temperatures. At each temperature, a 5-mm screw-capped NMR tube containing 0.042 g (0.058 mmol) of *cis*-**1** dissolved in 0.60 mL of 1,2-[D_2]tetrachloroethane was inserted into the NMR probe, which had been preheated at either 58, 68, 75, or 83 °C for 30 min. The sample was then thermally equilibrated in the probe for an additional 15 min after which quantitative ^{31}P{^{1}H} NMR spectra were taken at 5 min intervals. Concentrations of the *cis*- and *trans*-metallacrown ethers were calculated from the relative integrations of the ^{31}P{^{1}H} NMR resonances of the metallacrown ethers and the initial concentration of the metallacrown ether as discussed above. Plots of –ln(1 – [*trans*-

1]/[*trans*-**1**]$_e$) vs. time were linear and gave the reversible 1st-order rate constants for the forward reactions, k_f. The reversible 1st-order rate constants for the reverse reactions, k_r, were calculated from $K = k_f/k_r$ using the previously determined equilibrium constants.

For *trans*-**2**, a drop of a 12 M solution of DCl in D_2O was added to a solution of 0.042 g (0.053 mmol) of *trans*-**2** in 0.60 mL of 1,2-[D_2]-tetrachloroethane in a 5 mm, screw-capped NMR tube under an inert atmosphere. The tube was then inserted into the NMR probe, which had been preheated at 75 °C for 30 min. The sample was then thermally equilibrated in the probe for an additional 15 min after which quantitative $^{31}P\{^1H\}$ NMR spectra were taken at 20 min intervals. Concentrations of the *cis*- and *trans*-metallacrown ethers were calculated from the relative integrations of the $^{31}P\{^1H\}$ NMR resonances of the metallacrown ethers. A plot of [*trans*-**2**] vs. time was linear and gave the zero-order rate constant.

Eyring Analysis: Plots of $\ln(k_f/T)$ vs. $(1/T)$ using the rate constants obtained at the four temperatures for *cis*-**1** gave the $\Delta H^‡$ (slope) and $\Delta S^‡$ (intercept) for the forward reaction while plots of $\ln(k_r/T)$ vs. $(1/T)$ using the rate constants obtained at the four temperatures for *cis*-**1** gave the $\Delta H^‡$ (slope) and $\Delta S^‡$ (intercept) for the reverse reaction. Both plots were linear with r values greater than 0.995. Errors for the kinetic parameters were determined from linear least-squares analyses of the data.

Supporting Information (see also the footnote on the first page of this article): Thermodynamic and kinetic data for isomerizations.

Acknowledgments

The authors thank the Petroleum Research Fund, ACS PRF#35349-AC3, for partial financial support of this project. D. C. S. Jr. and S. B. O. Jr. also thank the Graduate School at the University of Alabama at Birmingham for support through a graduate fellowship.

[1] J. P. Collman, *Principles and applications of organotransition metal chemistry*, 2nd ed., University Science Books, Mill Valley, California, **1987**.
[2] T. G. Appleton, F. J. Pesch, M. Wienken, S. Menzer, B. Lippert, *Inorg. Chem.* **1992**, *31*, 4410.
[3] M. J. Coyer, R. H. Herber, J. Chen, M. Croft, S. P. Szu, *Inorg. Chem.* **1994**, *33*, 716.
[4] M. J. Coyer, M. Croft, J. Chen, R. H. Herber, *Inorg. Chem.* **1992**, *31*, 1752.
[5] Y. J. You, J. T. Chen, M. C. Cheng, Y. Wang, *Inorg. Chem.* **1991**, *30*, 3621.
[6] F. M. Macdonald, P. J. Sadler, *Polyhedron* **1991**, *10*, 1443.
[7] I. J. B. Lin, C. P. Chang, *J. Chin. Chem. Soc. (Taipei, Taiwan)* **1986**, *33*, 273.
[8] H. Tobita, H. Habazaki, H. Ogino, *Bull. Chem. Soc. Jpn.* **1987**, *60*, 797.
[9] M. Kotowski, R. van Eldik, *Stud. Inorg. Chem.* **1986**, *7*, 219.
[10] J. Mink, P. L. Goggin, *Kem. Kozl.* **1982**, *57*, 161.
[11] Y. N. Kukushkin, *Koord. Khim.* **1982**, *8*, 201.
[12] G. K. Anderson, R. J. Cross, *Inorg. Chem.* **1981**, *20*, 4459.
[13] V. G. Pogareva, *Koord. Khim.* **1981**, *7*, 1101.
[14] W. J. Louw, R. Van Eldik, *Inorg. Chem.* **1981**, *20*, 1939.
[15] R. Romeo, D. Minniti, S. Lanza, *Congr. Naz. Chim. Inorg. [Atti]*, 12th, **1979**, 315.
[16] G. K. Anderson, R. J. Cross, *Chem. Soc. Rev.* **1980**, *9*, 185.
[17] R. Romeo, D. Minniti, S. Lanza, *Inorg. Chem.* **1980**, *19*, 3663.
[18] M. K. Cooper, J. M. Downes, *Inorg. Chem.* **1978**, *17*, 880.
[19] C. E. Scott, S. H. Mastin, *Thermochim. Acta* **1976**, *14*, 141.
[20] D. A. Redfield, J. H. Nelson, *J. Am. Chem. Soc.* **1974**, *96*, 6219.
[21] E. A. Allen, J. Del Gaudio, W. Wilkinson, *Thermochim. Acta* **1975**, *11*, 197.
[22] D. A. Redfield, J. H. Nelson, R. A. Henry, D. W. Moore, H. B. Jonassen, *J. Am. Chem. Soc.* **1974**, *96*, 6298.
[23] D. A. Redfield, J. H. Nelson, *Inorg. Chem.* **1973**, *12*, 15.
[24] G. Alibrandi, L. Monsu Scoloaro, R. Romeo, *Inorg. Chem.* **1991**, *30*, 4007.
[25] W. E. Hill, D. M. A. Minahan, J. G. Taylor, C. A. McAuliffe, *J. Am. Chem. Soc.* **1982**, *104*, 6001.
[26] N. W. Alcock, T. J. Kemp, F. L. Wimmer, *J. Chem. Soc., Dalton Trans.* **1981**, 635.
[27] A. W. Verstuyft, J. H. Nelson, *Inorg. Chem.* **1975**, *14*, 1501.
[28] D. A. Redfield, L. W. Cary, J. H. Nelson, *Inorg. Chem.* **1975**, *14*, 50.
[29] D. A. Redfield, J. H. Nelson, *Inorg. Nucl. Chem. Lett.* **1974**, *10*, 931.
[30] D. G. Cooper, J. Powell, *Can. J. Chem.* **1973**, *51*, 1634.
[31] D. G. Cooper, J. Powell, *J. Am. Chem. Soc.* **1973**, *95*, 1102.
[32] J. Powell, D. G. Cooper, *J. Chem. Soc., Chem. Commun.* **1973**, 486.
[33] P. Haake, R. M. Pfeiffer, *J. Chem. Soc. C* **1969**, 1330.
[34] P. Haake, R. M. Pfeiffer, *J. Am. Chem. Soc.* **1970**, *92*, 4996.
[35] R. Favez, R. Roulet, A. A. Pinkerton, D. Schwarzenbach, *Inorg. Chem.* **1980**, *19*, 1356.
[36] M. Cusumano, G. Guglielmo, V. Ricevuto, S. Sostero, O. Traverso, T. J. Kemp, *J. Chem. Soc., Dalton Trans.* **1981**, 302.
[37] D. G. Cooper, Ph. D. Thesis, University of Toronto, Toronto, Canada, **1976**.
[38] D. C. Smith, C. H. Lake, G. M. Gray, *Dalton Trans.* **2003**, 2950.
[39] D. C. Smith, G. M. Gray, *J. Chem. Soc., Dalton Trans.* **2000**, 677.
[40] D. C. Smith, G. M. Gray, *Inorg. Chem.* **1998**, *37*, 1791.
[41] A. Varshney, M. L. Webster, G. M. Gray, *Inorg. Chem.* **1992**, *31*, 2580.
[42] A. Varshney, G. M. Gray, *Inorg. Chem.* **1991**, *30*, 1748.
[43] G. M. Gray, *Comments Inorg. Chem.* **1995**, *17*, 95.
[44] G. M. Gray, C. H. Duffey, *Organometallics* **1995**, *14*, 245.
[45] G. M. Gray, A. Varshney, C. H. Duffey, *Organometallics* **1995**, *14*, 238.
[46] G. M. Gray, F. P. Fish, C. H. Duffey, *Inorg. Chim. Acta* **1996**, *246*, 229.
[47] G. M. Gray, D. C. Smith, C. H. Duffey, *Inorg. Chim. Acta* **2000**, *300*, 581.
[48] D. F. Shriver, P. W. Atkins, *Inorganic Chemistry*, 3rd ed., W. H. Freeman, Co., New York, **1999**, p. 469–471.
[49] A. Dedieu, *Chem. Rev.* **2000**, *100*, 543.
[50] P. B. Dias, M. E. M. Depiedade, J. A. M. Simoes, *Coord. Chem. Rev.* **1994**, *135*, 737.
[51] G. Pacchioni, P. S. Bagus, *Inorg. Chem.* **1992**, *31*, 4391.
[52] T. R. Cundari, J. Deng, Y. Zhao, *THEOCHEM* **2003**, *632*, 121.
[53] G. A. Takhin, H. A. Skinner, A. A. Zaki, *J. Chem. Soc., Dalton Trans.* **1984**, 371.
[54] M. S. Kharasch, R. C. Seyler, F. R. Mayo, *J. Am. Chem. Soc.* **1938**, *60*, 882.
[55] J. R. Doyle, P. E. Slade, H. B. Jonassen, *Inorg. Synth.* **1960**, *6*, 216.
[56] G. M. Sheldrick, *SHELXTL6.1*, Bruker AXS, Madison, WI, **2000**.
[57] A. L. Spek, *PLATON/SQUEEZE—an effective tool for taking the contribution of disordered solvent into account in crystal structure refinement*, Bijvoet Center for Biommolcular Research, Utrecht University, The Netherlands, **2004**.
[58] P. Van der Sluis, A. L. Spek, *Acta Crystallogr., Sect. A: Found. Crystallogr.* **1990**, *46*, 194.

Received: April 28, 2008
Published Online: September 10, 2008

